animal research of the Tokyo University. Streptozotocin (STZ; 50 mg/kg body weight; Sigma-Aldrich) was dissolved in citrate buffer (pH 4.5) and injected in the tail vein of male Wistar rats (6 weeks old; Charles River, Wilmington, MA, USA). Blood glucose level was measured 4 weeks later to confirm that these rats had become diabetic. Adenovirus suspension diluted in saline up to 200 μL was injected into the penis 6 weeks after STZ injection. Adenovirus expressing green fluorescent protein (AdGFP), adrenomedullin (AdAM), angiopoietin-1 (AdAng-1), or vascular endothelial growth factor-A (AdVEGF-A) was injected into the penis (10 rats per group). Furthermore, AdAM plus AdAng-1 or AdVEGF-A plus AdAng-1 was injected into the penis (10 rats per group). Four weeks after adenovirus injection, rats (16 weeks old) were subjected to intracavernous pressure (ICP) measurement. The penis was also harvested for histochemical analysis and Western blot analysis at this time point. The penises isolated from six rats per group were subjected to ICP measurements, and then Western blot analysis. The penises isolated from the remaining four rats per group were used for histochemical analysis. AdGFP-injected diabetic rats were used as negative controls, and age-matched nondiabetic Wistar rats were used as positive controls in this study.

ICP Measurement

ICP measurement was performed in the same way as we previously reported [16]. Rats were anesthetized with ketamine (100 mg/kg body weight) injected intraperitoneally. The left carotid artery was exposed and cannulated with a PE-50 polyethylene tube to continuously monitor mean arterial pressure (MAP). The penis was denuded of skin and the pelvic nerve and cavernous nerve were isolated. The right cavernous nerve was hooked with stainless platinum bipolar electrodes (Unique Medical Co., Tokyo, Japan) and connected to a nerve stimulator (Nihon Kohden Co., Tokyo, Japan). Unilateral electrical field stimulation of the cavernous nerve was performed for 10 seconds using a square wave stimulator. The magnitude of the electrical voltage was 5.0 V with a pulse duration of 2 msec, and the frequency of the stimulation was 20 Hz. The right cavernous body was cannulated with a 23-gauge needle connected to a pressure transducer to continuously monitor ICP. Area under the curve (AUC) of ICP traces as well as the ratio of peak ICP to MAP (ICP/MAP) were used to evaluate erectile function. AUC was measured from the point when ICP started to increase from the base line values after electrical stimulation to the point when ICP decreased and reached a plateau. ICP × time was integrated every 0.2 second to calculate AUC.

Protein Extraction and Western Blot Analysis

The penis was homogenized in a cell lysis buffer (50 mM Tris-HCl [pH 8.0], 150 mM NaCl, 1% NP-40) containing 2 μg/mL aprotinin, 2 μg/mL leupeptin, and 1 mM phenylmethylsulfonyl fluoride. Western blot analysis was performed as previously described [17]. To detect type I collagen, we performed electrophoresis under nondenatured conditions, because the anti-type I collagen antibody used in this experiment recognizes nondenatured protein. Sodium dodecyl sulfate (SDS) and β-mercaptoethanol were left out from the loading dye, and samples were loaded on polyacrylamide gel without boiling. SDS was also omitted from the polyacrylamide gel, electrophoresis buffer, and transfer buffer. The expression of VE-cadherin, SMA, and type I collagen was normalized by calculating the ratio of the expression of those proteins to that of β-actin.

RNA Extraction and Real Time PCR Analysis

Total RNA was extracted using TRIZOL Reagent (Gibco-BRL, Rockville, MD, USA) according to the instructions provided by the manufacturer. To extract total RNA from the rat penis, the penis was homogenized in the TRIZOL Reagent. Total RNA was subjected to reverse transcription using a ReverTra Ace qPCR RT Kit (Toyobo, Osaka, Japan). Expression of rat AM, Ang-1, VEGF-A and glyceraldehyde 3-phosphate dehydrogenase (GAPDH) was examined by real-time PCR using an SYBR Green dye (Thunderbird SYBR qPCR Mix, Toyobo). Primers used were as follows:

RatAMsense, 5′-GCAGTTCCGAAAGAAGTG GAAT-3′
RatAMantisense, 5′-GCTGCTGGACGCTTGT AGTTC-3′
RatAng-1sense, 5′-CAGGAGGTTGGTGGTT TGATG-3′
RatAng-1antisense, 5′-TTTGCCCTGCAGTG TAGAACATT-3′
RatVEGF-Asense, 5′-GAGTATATCTTCAAGC CGTCCTGTGT-3′
RatVEGF-Aantisense, 5′-TCCAGGGCTTCAT CATTGC-3′
RatGAPDHsense, 5′-GTATGACTCTACCCAC GGCAAGT-3′
RatGAPDHantisense, 5′-TTCCCGTTGATGA CCAGCTT-3′

Real-time PCR was performed using an ABI PRISM 7000 sequence detection system (Applied Biosystems, Foster City, CA, USA). To confirm that no significant amounts of primer dimers were formed, dissociation curves were analyzed.

Histochemistry

The penis was fixed by perfusing it with 4% paraformaldehyde and then processed for paraffin embedding. Cross sections (5 μm) were cut, deparaffinized, rehydrated, and subjected to Elastica van Gieson stain to visualize collagen and elastin fibers in the trabeculae of the cavernous body. For immunohistochemistry, sections were incubated with a primary antibody reactive to VE-cadherin and SMA. Sections were then incubated with biotinylated secondary antibody and finally horseradish peroxidase-labeled streptavidin according to the instructions provided by the manufacturer (DAKO, Cambridgeshire, UK).

Construction of Adenovirus that Expresses VEGF-A

Replication-defective adenovirus that expresses rat VEGF-A was constructed according to the method described previously using an AdMax kit (Microbix Biosystems Inc., Ontario, Canada) [18]. The coding region of rat VEGF-A was amplified by PCR and subcloned into the pDC516 vector. The primer sequences used for PCR were as follows:

RatVEGF-Asense primer: 5′-ATGAACTTTCT GCTCTCTTGGGT-3′
RatVEGF-Aantisense primer: 5′-TCACCGCCT TGGCTTGTCACAT-3′

The result of DNA sequencing analysis showed that the VEGF-A isolated in this study was rat VEGF-A164 corresponding to human VEGF-A165, in which amino acids 141 to 164 were missing by alternative splicing. The expression plasmid pDC516 that expresses rat VEGF-A164 was cotransfected into HEK293 cells with pBHGfrtdelE13FLP to construct an adenovirus expressing rat VEGF-A164 (AdVEGF-A). Construction of adenovirus that expresses rat AM (AdAM) [4] and rat Ang-1 (AdAng-1) [19] has been reported elsewhere. Recombinant adenovirus that expresses GFP (AdGFP) was obtained from Quantum Biotechnologies (Montreal, Canada). These adenoviruses were purified before in vivo use with the Adeno-X Maxi Purification Kit (Takara Bio Inc., Tokyo, Japan) according to the manufacturer's instructions.

Enzyme-Linked Immunosorbent Assay

Rat VEGF-A in culture medium was measured with an enzyme-linked immunosorbent assay kit (Abcam, Cambridge, UK) according to the methods provided by the manufacturer.

Statistical Analysis

The values are expressed as the mean ± SEM. Statistical analyses were performed using analysis of variance followed by the Student–Neumann–Keuls test. Differences with a P value of <0.05 were considered statistically significant.

Results

Characterization of AdVEGF-A

We first examined whether AdVEGF-A-infected cells produced VEGF-A using an ELISA kit for rat VEGF-A. We infected NRK-52E cells with AdVEGF-A and measured the VEGF-A content in the culture medium. Although we expected that the NRK-52E cells did not produce endogenous VEGF-A, they produced a significant amount of VEGF-A (Figure 1). However, AdVEGF-A-infected NRK-52E cells produced a more significant amount of VEGF-A (approximately fivefolds) compared with the AdGFP-infected and noninfected control NRK-52E cells, confirming that the AdVEGF-A used in this study produced VEGF-A protein. Previous studies have reported that

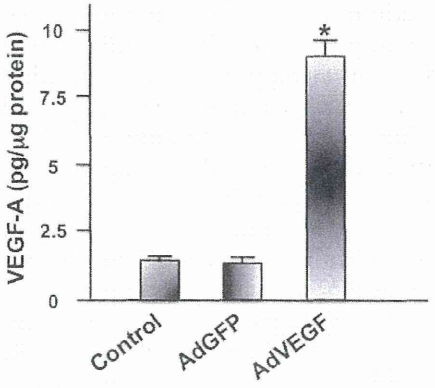

Figure 1 Production of VEGF-A by AdVEGF-A. NRK-52E cells were cultured in 24-well plates and infected with AdGFP or AdVEGF-A for 3 days. After washing the wells with phosphate-buffered saline (PBS), medium was replaced with serum-free DMEM, and incubated for 2 hours. VEGF-A accumulated in the medium was measured with an ELISA kit. Noninfected NRK 52E cells were also used as the control (Control). *: $P < 0.001$ vs. control and AdGFP infection ($n = 6$ each)

AdAM produces rat AM protein [4] and AdAng-1 produces rat Ang-1 protein [19].

Expression of Adenovirus in the Penis

To confirm that adenovirus injected into the penis expressed AM, Ang-1, and VEGF-A in the penis, AdGFP, AdAM, AdAng-1, or AdVEGF-A were injected into the penis of STZ-induced diabetic rats, and the penis was harvested 7 days after adenoviral infection for real-time PCR analysis. Penises injected with AdAM, AdAng-1, and AdVEGF-A expressed significantly higher amounts of AM, Ang-1, and VEGF-A, respectively, than those injected with AdGFP. This result suggested that adenovirus injected into the penis remained and those cytokines were therefore expressed (Figure 2).

Effects of Administration of AdAM, AdAng-1, and AdVEGF-A on ICP

We infected AdAM, AdAng-1, and AdVEGF-A into the cavernous body at the glans of STZ-induced diabetic rats and measured ICP 4 weeks after the infection. We confirmed in a previous study that AdGFP infection did not affect ICP or histology in STZ-induced diabetic rats [4]. We analyzed not only ICP and AUC of ICP traces, but also Tmax and $T_{1/2}$. Tmax is defined as a period from when ICP starts to increase after electrical stimulation to when ICP reaches maximal level (Figure 3A). $T_{1/2}$ is defined as a period from when ICP starts to increase after electrical stimulation to when ICP decreases to the 50% level of its maximal value (Figure 3A). Infection of the penis with AdAM, AdAng1, AdAM plus AdAng-1, AdVEGF-A, and AdVEGF-A plus AdAng-1 all restored ICP significantly compared with AdGFP infection in the diabetic rats (Figure 3B). Infection with AdAM plus AdAng-1, AdVEGF-A, and AdVEGF-A plus AdAng-1 restored ICP to a level similar to that observed in age-matched Wistar rats (positive control). Infection with AdAM, AdAng1, AdAM plus AdAng-1, AdVEGF-A, and AdVEGF-A plus AdAng-1 also increased AUC of the ICP traces significantly compared with AdGFP infection in the diabetic rats (Figure 3C). Infection with AdAM plus AdAng-1 restored AUC most significantly. Tmax in the AdGFP-infected group was significantly elongated compared with the positive control group (Figure 3D), and Tmax in the AdAng-1-infected group tended to be retarded, and there was no significant difference in Tmax between the AdGFP-infected group and the AdAng-1-infected group. These results suggested

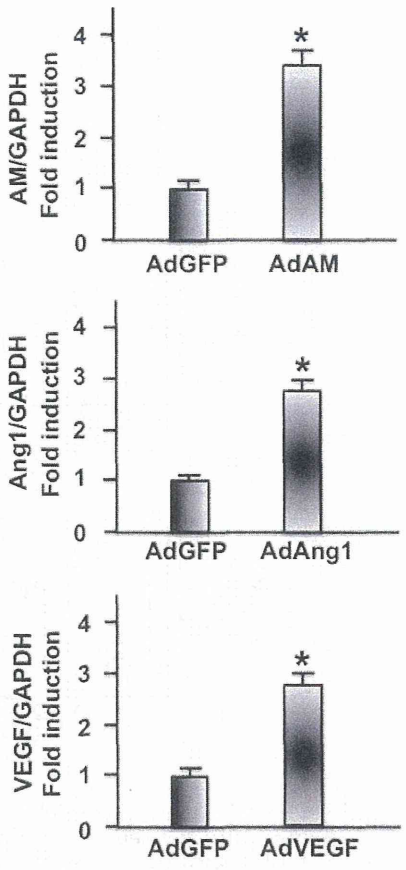

Figure 2 Expression of adenovirus in the penis. AdAM, AdAng-1, or AdVEGF-A was injected into the penis of STZ-induced diabetic rats, and the penis was isolated 7 days after adenoviral injection for real-time PCR analysis. AdGFP was also injected into the penis as a negative control. Expression of AM, Ang-1, and VEGF-A (VEGF) was normalized by that of GAPDH ($n = 4$ each). *: $P < 0.01$ vs. AdGFP infection

that blood filling into the cavernous body occurred more slowly in the AdGFP-infected and AdAng-1-infected diabetic rats than the age-matched Wistar rats. Interestingly, Tmax in the AdVEGF-A- and AdVEGF-A plus AdAng-1-infected groups was significantly shortened compared with the positive control group, suggesting that blood filling into the cavernous body occurred faster in these groups than the positive control. Tmax in the AdAM- and AdAM plus AdAng-1-infected groups was similar to that in the positive control group. $T_{1/2}$ in the AdGFP- and AdAng-1-infected groups was significantly elongated compared with the positive control (Figure 3E). $T_{1/2}$ in the AdVEGF-A- and AdVEGF-A plus AdAng-1-infected groups was significantly shortened

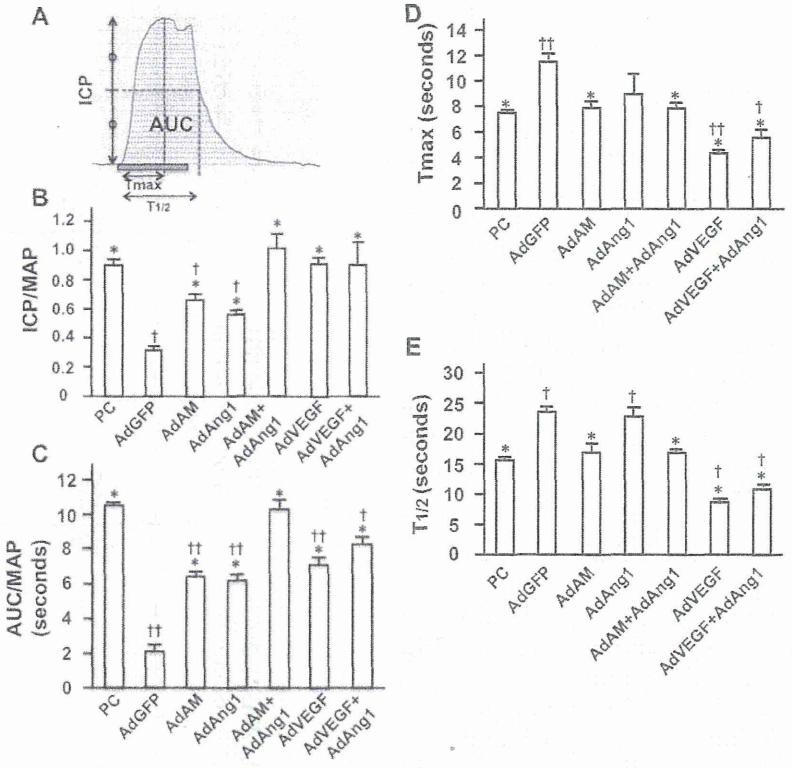

Figure 3 Effects of AdAM, AdAng-1, and AdVEGF-A infection on erectile function. These adenoviruses were infected into the cavernous body of STZ-induced diabetic rats. Age-matched Wistar rats were used as the positive control (PC). (A) Schematic representation of ICP traces. The dashed box indicates the timing and duration of electrical stimulation. The dotted area represents AUC. Tmax was defined as the period from when ICP started to rise to when ICP reached its peak level. $T_{1/2}$ was defined as the period from when ICP started to rise to when it fell to the 50% of its peak level. (B) Bar graphs comparing ICP/MAP among the groups ($n = 6$ each). *: $P < 0.001$ vs. AdGFP infection and †: $P < 0.001$ vs. PC. (C) Bar graphs comparing AUC/MAP among the groups ($n = 6$ each). *: $P < 0.001$ vs. AdGFP infection, and † and ††: $P < 0.01$ and $P < 0.001$, respectively, vs. PC. (D) Bar graphs comparing Tmax among the groups ($n = 6$ each). *: $P < 0.001$ vs. AdGFP infection and † and ††: $P < 0.05$ and $P < 0.001$, respectively vs. PC. (E) Bar graphs comparing $T_{1/2}$ among the groups ($n = 6$ each). *: $P < 0.001$ vs. AdGFP infection and †: $P < 0.001$ vs. PC

compared with the positive control group. $T_{1/2}$ in the AdAM- and AdAM plus AdAng-1-infected groups was similar to that in the positive control group. Collectively, infection with AdAM, AdAng1, AdAM plus AdAng-1, AdVEGF-A, and AdVEGF-A plus AdAng-1 all restored erectile function significantly. The effect of AdAM plus AdAng-1 infection was most significant, and the erectile function in this group was similar to that in the positive control group. The speed of rise and fall of ICP after electrical stimulation was decreased in the AdGFP- and AdAng-1-infected groups compared with the positive control group. The speed increased in the AdVEGF-A- and AdVEGF-A plus AdAng-1-infected groups compared with the positive control group. The speed did not change significantly in the AdAM- or AdAM plus AdAng-1-infected group compared with the positive control group. Thus, ICP traces in the AdAM plus AdAng-1-infected group mostly mimicked those in the positive control group.

Effects of Administration of AdAM, AdAng-1, and AdVEGF-A on Histology of the Cavernous Body

To examine the mechanisms by which these adenoviral infections restored erectile function, we examined the morphology of the cavernous body by Elastica van Gieson staining. The trabeculae of the cavernous body at the root of the penis in the AdGFP-infected diabetic rats were smaller than those in the positive control Wistar rats (Figure 4). Infection with AdAM and/or AdAng-1 restored the size of the trabeculae of the cavernous body.

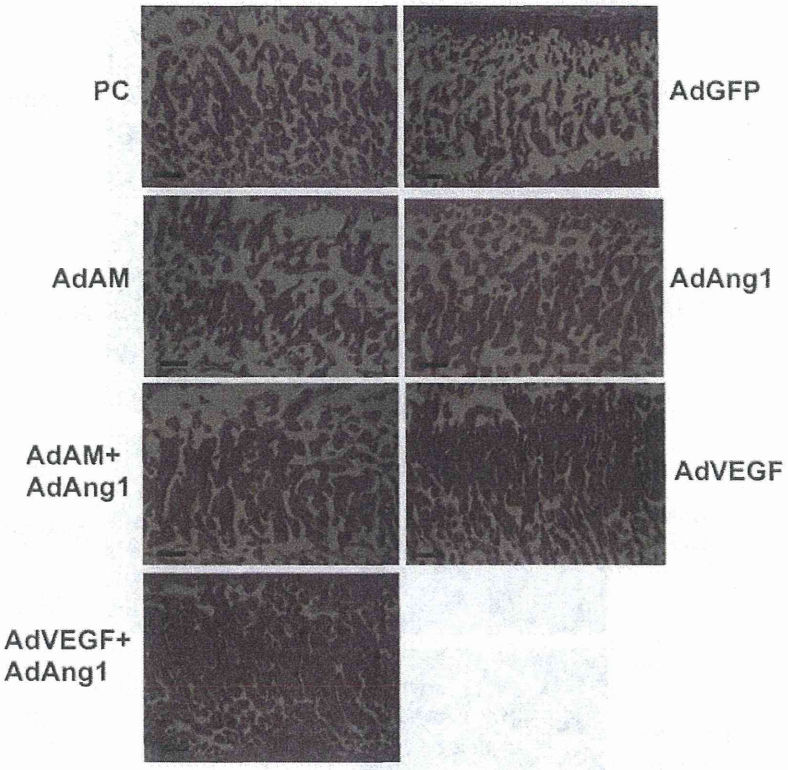

Figure 4 Histological analysis of the cavernous body after adenoviral infection. Elastica van Gieson staining of the cavernous body isolated from age-matched Wistar rats (PC), and STZ-induced diabetic rats infected with AdGFP, AdAM, AdAng-1, AdAM plus AdAng-1, AdVEGF-A (AdVEGF), and AdVEGF-A plus AdAng-1. The histology of the root portion of the penis (longitudinal section) is shown. Bars are 300 μm.

Interestingly, the trabeculae of the cavernous body were rather enlarged and densely distributed in the cavernous body in the AdVEGF-A- and AdVEGF-A plus AdAng-1-infected groups compared with the positive control group. We next examined the distribution of SMA and VE-cadherin by immunohistological analysis. The SMA layer around the trabeculae of the cavernous body in the AdGFP-infected diabetic rats looked thinner than that in the other adenovirus-infected groups and the positive control group (Figure 5). The VE-cadherin-positive endothelial layer around the trabeculae of the cavernous body was observed in all groups (Figure 6), and the ratios of trabeculae covered with VECs to those uncovered with VECs seemed to be similar among the groups, although the total amount of the endothelial layer might be different among the groups because the size and the density of the trabeculae of the cavernous body differed among the groups. Interestingly, we observed a VE-cadherin-positive tube-like structure in the trabeculae of the cavernous body in the AdVEGF-A-infected group (Figure 6), suggesting that an aberrant angiogenesis occurred in the AdVEGF-A-infected group.

Effects of Administration of AdAM, AdAng-1, and AdVEGF-A on the Expression of VE-Cadherin, SMA, and Type I Collagen

To quantify the expression of SMA and VE-cadherin, we performed Western blot analysis (Figure 7). Infection with AdAM or AdAng-1 increased SMA expression slightly but significantly compared with AdGFP infection. Infection with AdAM plus AdAng-1, AdVEGF-A, and AdVEGF-A plus AdAng-1 increased SMA expression more significantly, and the expression level was similar to that in the age-matched positive control group. Infection with AdAM or AdAng-1 significantly increased VE-cadherin expression compared with AdGFP infection. Infection with AdAM plus AdAng-1 increased VE-cadherin expression more significantly, and the expression reached a level similar to that in the positive control group. The expression of VE-cadherin in the AdVEGF-A- and AdVEGF-A plus AdAng-1-infected groups rather surpassed the expression level observed in the positive control. We also examined the expression of type I collagen as a marker to quantify the content of collagen fibers in the trabeculae of the cavernous body, because we found that the trabeculae were "hypertrophied" in

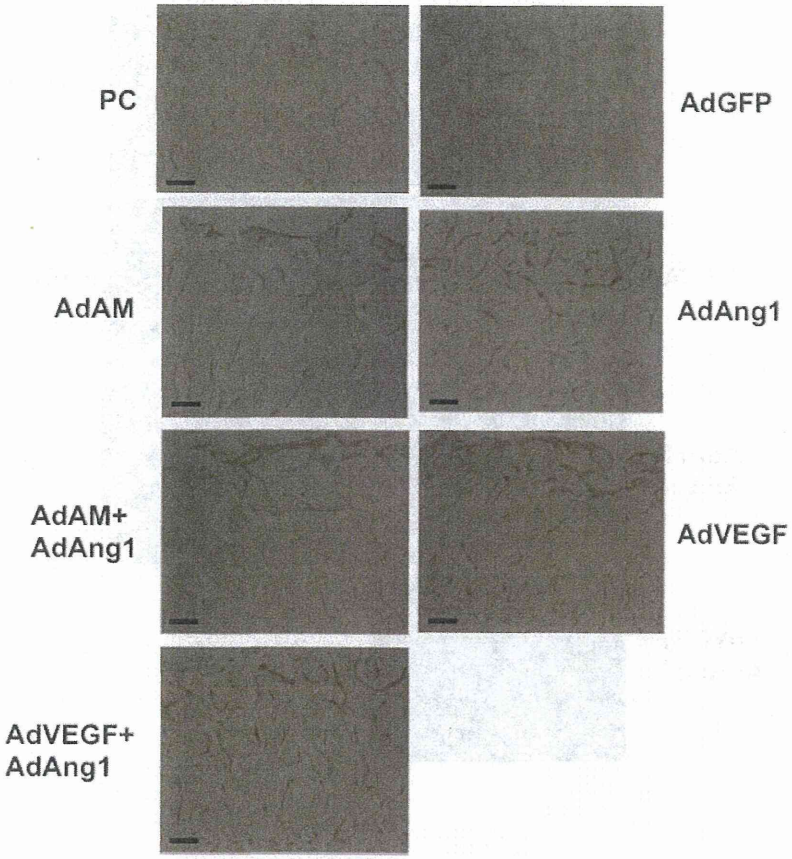

Figure 5 Immunohistochemical analysis of the cavernous body isolated from age-matched Wistar rats (PC) and STZ-induced diabetic rats infected with AdGFP, AdAM, AdAng-1, AdAM plus AdAng-1, AdVEGF-A (AdVEGF), and AdVEGF-A plus AdAng-1. SMA was stained to visualize the smooth muscle layer in the cavernous body. The longitudinal section of the cavernous body at the root of the penis is shown. Bars are 300 μm.

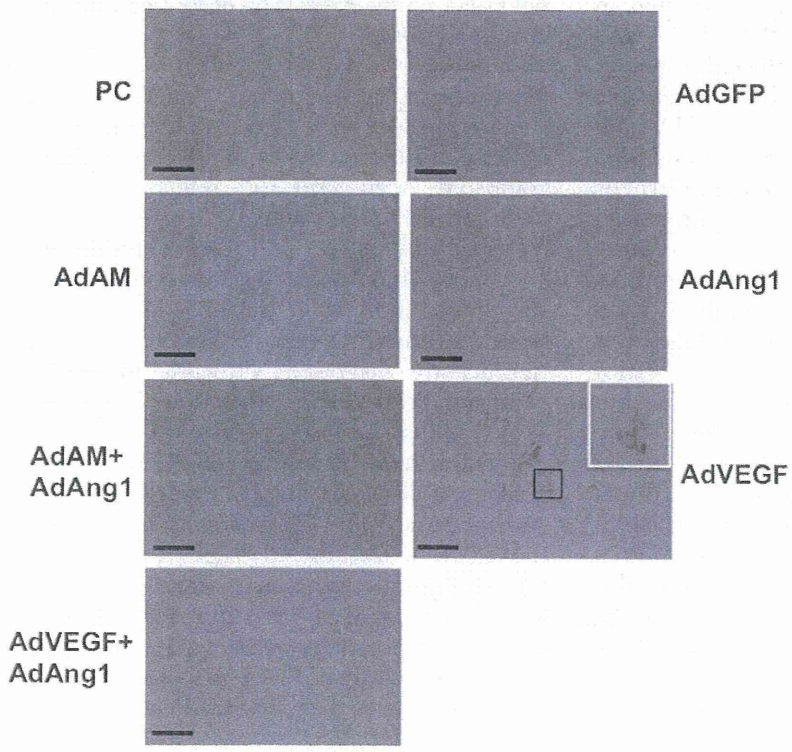

Figure 6 Immunohistochemical analysis of the cavernous body isolated from age-matched Wistar rats (PC) and STZ-induced diabetic rats infected with AdGFP, AdAM, AdAng-1, AdAM plus AdAng-1, AdVEGF-A (AdVEGF), and AdVEGF-A plus AdAng-1. VE-cadherin was stained to visualize the endothelial layer in the cavernous body. Area of aberrant angiogenesis observed in the trabeculae of the cavernous body of AdVEGF-A infected penis was boxed and enlarged in the white box. The longitudinal section of the cavernous body at the root of the penis is shown. Bars are 100 μm.

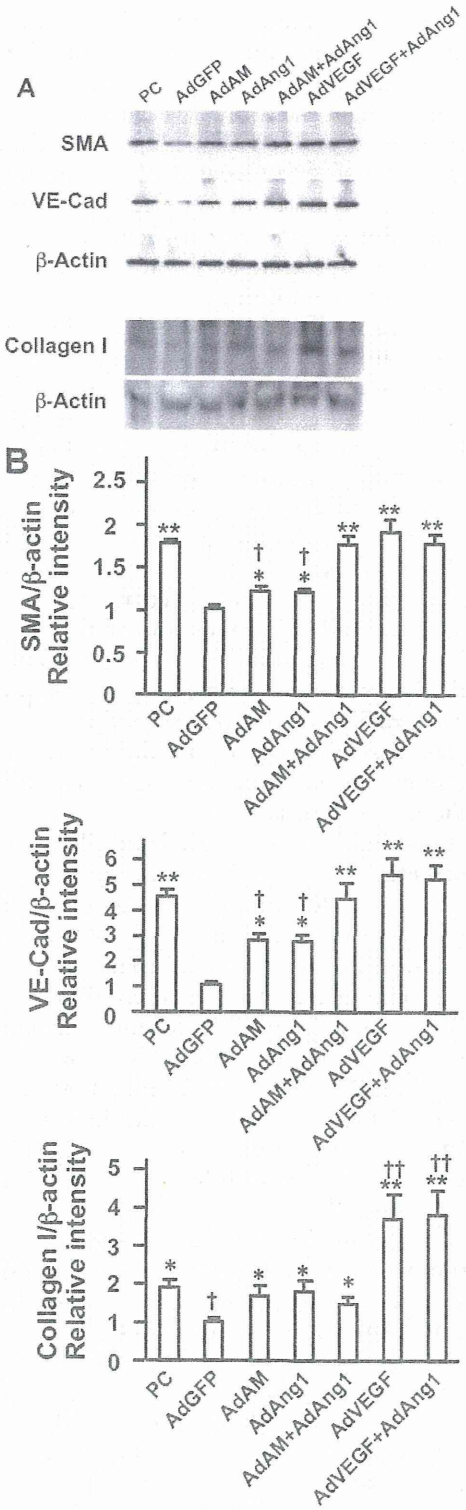

Figure 7 Western blot analysis of the expressions of SMA, VE-cadherin, and type I collagen in the penis. (A) AdGFP, AdAM, AdAng-1, AdAM plus AdAng-1, AdVEGF-A (AdVEGF), and AdVEGF-A plus AdAng-1 were infected in the cavernous body of STZ-treated diabetic rats, and the penis was isolated for protein extraction 4 weeks after adenoviral injection. Age-matched Wistar rats were used as the positive control (PC). The blotted membranes were incubated with anti-SMA antibody, anti-VE-cadherin antibody, and then anti-β-actin antibody as the internal control. To detect type I collagen, protein extracts were electrophoresed on nondenatured SDS polyacrylamide gels, and blotted membranes were incubated with anti-type I collagen antibody and then anti-β-actin antibody as the internal control. (B) Histograms showing relative intensity of the bands ($n = 4$ each). * and **: $P < 0.05$ and $P < 0.01$ vs. AdGFP infection, and † and ††: $P < 0.05$ and $P < 0.01$, respectively, vs. PC.

the AdVEGF-A- and AdVEGF-A plus AdAng-1-infected groups. Expression level of type I collagen in the AdGFP-infected diabetic rats was significantly lower than that in the positive control. AdAM and/or AdAng-1 infection significantly restored the expression of type I collagen to a level similar to that in the positive control. Infection with AdVEGF-A and AdVEGF-A plus AdAng-1 further increased the expression of type I collagen, and the expression level significantly exceeded that in the positive control. Collectively, these results suggested that the vascular networks of the cavernous sinus were poorly developed in the AdGFP-infected diabetic rats, and infection with AdAM, AdAng-1, and AdVEGF-A restored the networks significantly. However, AdVEGF-A infection induced an excess amount of angiogenesis and synthesis of collagen fibers, resulting in aberrant angiogenesis in the trabeculae of the cavernous body and "hypertrophy" of the trabeculae.

Blood Glucose Levels Before and After Adenoviral Infection

To confirm that adenoviral infection did not affect blood glucose levels, we measured the casual blood glucose levels 4 weeks after STZ injection (before adenoviral infection) and 10 weeks after STZ injection (4 weeks after adenoviral infection). Adenoviral infection did not significantly alter the blood glucose levels, and the diabetic rats remained diabetic after the infection. The blood glucose levels of adenovirus-infected diabetic rats were significantly higher than age-matched nondiabetic rats (16 weeks old) (Supporting Information Figure S1).

Discussion

In this study, we found that overexpression of AM, Ang-1, and VEGF-A by adenoviral infection significantly restored erectile function in terms of ICP, histology of the penis, and expression of several proteins in the penis. Among several combinations, infection with AdAM plus AdAng-1 mostly mimicked the erectile function in the age-matched positive control. AdAM plus AdAng-1 infection restored ICP and AUC of the ICP traces to a similar level observed in the positive control. The pattern of the increase and decrease of ICP after electrical stimulation was similar between the AdAM plus AdAng-1-infected group and the positive control group. Expression of SMA and VE-cadherin was also similar between the AdAM plus AdAng-1-infected group and the positive control group. In contrast, although ICP rose sufficiently after electrical stimulation in the AdVEGF-A- and AdVEGF-A plus AdAng-1-infected groups, the rise and fall of ICP occurred more rapidly, as assessed by Tmax and $T_{1/2}$, resulting in a smaller value of AUC compared with the AdAM plus AdAng-1-infected group and the positive control. Infection with AdVEGF-A and AdVEGF-A plus AdAng-1 induced "hypertrophy" of the trabeculae of the cavernous body and overproduction of collagen fibers in the trabeculae. Infection with AdVEGF-A induced aberrant angiogenesis in the trabeculae. We propose the following scenario about the effect of AdVEGF-A- and AdVEGF-A plus AdAng-1-infection. Because the trabeculae of the cavernous body were "hypertrophied," the area of the cavernous sinus was relatively small in these rats. Therefore, once erection started, blood filled in the cavernous sinus rapidly, but once erection ceased, blood outflow from the cavernous sinus also occurred rapidly. That is why the level of ICP rose and fell rapidly in the AdVEGF-A- and AdVEGF-A plus AdAng-1-infected groups. Another possibility is that AdVEGF-A infection did not sufficiently improve corporal veno-occlusive dysfunction (CVOD). It is well known that CVOD is the most prevalent cause of ED. This disorder results from an inadequate relaxation of the corporal smooth muscle, resulting in insufficient compression of the subtunical veins against the tunica albuginea [20]. Decreases in the amount of smooth muscle cells (SMC) and/or increases in the amount of collagen in the cavernous body appear to result in dysfunction of the corporal smooth muscle and CVOD [21,22]. Infection with AdAM plus AdAng-1 restored the amount of SMC in the cavernous body without increases in the amount of collagen fibers, whereas infection with AdVEGF-A and AdVEGF-A plus AdAng-1 increased the amount of collagen as well as SMC. This may be the reason why the blood flowed out of the cavernous body rapidly after cessation of electrical stimulation in AdVEGF-A- and AdVEGF-A plus AdAng-1-infected groups compared with the AdAM plus AdAng-1-infected group.

Although VEGF are essential for vasculogenesis and have probably the most potent proangiogenic activity, overproduction of VEGF potentially causes a harmful effect on organ physiology [12,13]. In fact, it was reported that the VEGF-A gene transfer using the adeno-associated virus into rabbit ischemic hind limb skeletal muscles caused aberrant angiogenesis and fibrosis in skeletal muscles [23]. It was also reported that the blockade of the type 2 receptor for the VEGF family resulted in attenuation of fibrosis in the kidney in a unilateral ureteric obstruction model [24]. Therefore, it appears that an appropriate amount of VEGF-A is necessary for physiological angiogenesis and that overproduction of VEGF-A potentially causes aberrant angiogenesis, inflammation, and fibrosis.

Ang-1 reportedly restored erectile function in a diabetes model and a hyperlipidemia model [11,25]. In addition to proangiogenic activity, Ang-1 appears to have an inhibitory effect on fibrosis. It was shown that a variant of Ang-1 (cartilage oligomeric matrix protein-Ang-1) that is stable and has a potent activity, inhibited fibrosis in a unilateral ureteric obstruction model of the kidney [26]. Furthermore, Ang-1 reportedly inhibits tissue inflammation via suppression of macrophage infiltration and activation [27,28]. Thus, it seems to be reasonable to use Ang-1 for the treatment of ED.

AM was originally isolated from human pheochromocytoma tissue and has potent natriuretic, vasorelaxant, and proangiogenic activities [5–8]. We have shown that overproduction of AM in the penis restores erectile function via stimulation of the regeneration of the cavernous tissue and via restoration of endothelial function [4]. Furthermore, it was reported that AM inhibited tissue fibrosis in the heart and the kidney [29–31]. Thus, AM also has proangiogenic and antifibrotic activities like Ang-1. In this study, we found that infection with AdAM plus AdAng-1 in the penis restored erectile function more potently than infection with AdAM alone or AdAng-1 alone.

Expression of SMA and VE-cadherin in the penis increased more significantly in the AdAM plus AdAng-1-infected group than in the AdAM-infected and AdAng-1-infected group without overproduction of type I collagen. The expressions of SMA and VE-cadherin in the AdAM plus AdAng-1-infected group increased to a level similar to that observed in the positive control group. Thus, vascular networks in the cavernous sinus appear to be restored more significantly by AdAM plus AdAng-1-infection than by AdAM infection alone or AdAng-1 infection alone. This can be a mechanism whereby AM and Ang-1 additively restore erectile function. Another possible mechanism is that AM and Ang-1 additively restored vascular endothelial function. In fact, we have reported that AM stimulates phosphorylation and activation of endothelial nitric oxide synthase (eNOS) in the penis [4]. Another study reported that Ang-1 stimulates phosphorylation of eNOS in the penis [11]. Furthermore, AM and Ang-1 reportedly inhibit the production of reactive oxygen species (ROS) [32,33]. As it has been shown that ROS are implicated in ED in diabetes [34,35], AM and Ang-1 may restore erectile function via suppression of ROS production. Therefore, it is possible that AM and Ang-1 additively restores erectile function via improvement of vascular endothelial function by activating eNOS and/or suppressing ROS production in an additive manner. Future studies are required to elucidate these possibilities.

Limitations of This Study

Adenovirus was injected into the penis. Thus, some portions of the injected adenovirus may have entered the systemic circulation and got trapped in the tissues of organs such as the liver, which may then have produced AM, Ang-1, or VEGF-A. These cytokines produced outside the penis may have entered the systemic circulation and affected the results of this study. However, we believe that this effect was minimal, if present at all, because no decline in blood pressure was observed after injection of AdAM into the penis (data not shown). Because AM has a potent vasodilator activity, blood pressure should have decreased if systemically delivered adenovirus played a major role in erectile function.

AM, Ang-1, and/or VEGF-A may have also improved erectile function through regenerative effects on the autonomic nervous system. This possibility should be addressed in a future study.

Conclusions

Combination therapy with AM and Ang-1 additively restored erectile function to a level very similar to that observed in the age-matched Wistar rats. This combination therapy effectively regenerated vascular structure in the cavernous body without inducing aberrant angiogenesis, overproduction of collagens and "hypertrophy" of the trabeculae of the cavernous body. This combination therapy will be useful to treat ED resulting from old age and diabetes.

Acknowledgment

This study was supported in part by Grants-in-Aid #21592066 and #24592423 (to H. N.) from the Ministry of Education, Culture, Sports, Science and Technology of Japan.

Corresponding Author: Etsu Suzuki, MD, PhD, Institute of Medical Science, St. Marianna University School of Medicine, 2-16-1 Sugao, Miyamae-ku, Kawasaki 216-8512, Japan. Tel: +81-44-977-8111; Fax: +81-44-977-8361; E-mail: esuzuki-tky@umin.ac.jp

Conflict of Interest: The author(s) report no conflicts of interest.

Statement of Authorship

Category 1

(a) **Conception and Design**
Etsu Suzuki; Hiroaki Nishimatsu; Yukio Homma

(b) **Acquisition of Data**
Etsu Suzuki; Hiroaki Nishimatsu; Akira Nomiya; Aya Niimi; Motofumi Suzuki; Tetsuya Fujimura; Hiroshi Fukuhara

(c) **Analysis and Interpretation of Data**
Etsu Suzuki; Hiroaki Nishimatsu; Akira Nomiya; Aya Niimi

Category 2

(a) **Drafting the Article**
Etsu Suzuki; Hiroaki Nishimatsu; Yukio Homma

(b) **Revising It for Intellectual Content**
Akira Nomiya; Aya Niimi; Motofumi Suzuki; Tetsuya Fujimura; Hiroshi Fukuhara

Category 3

(a) **Final approval of the completed article**
Etsu Suzuki; Hiroaki Nishimatsu; Akira Nomiya; Aya Niimi; Motofumi Suzuki; Tetsuya Fujimura; Hiroshi Fukuhara; Yukio Homma

References

1 Malavige LS, Levy JC. Erectile dysfunction in diabetes mellitus. J Sex Med 2009;6:1232–47.

2 Dey J, Shepherd MD. Evaluation and treatment of erectile dysfunction in men with diabetes mellitus. Mayo Clin Proc 2002;77:276–82.
3 Siroky MB, Azadzoi KM. Vasculogenic erectile dysfunction: Newer therapeutic strategies. J Urol 2003;170:S24–30.
4 Nishimatsu H, Suzuki E, Kumano S, Nomiya A, Liu M, Kume H, Homma Y. Adrenomedullin mediates adipose tissue-derived stem cell-induced restoration of erectile function in diabetic rats. J Sex Med 2012;9:482–93.
5 Kitamura K, Kangawa K, Kawamoto M, Ichiki Y, Nakamura S, Matsuo H, Eto T. Adrenomedullin: A novel hypotensive peptide isolated from human pheochromocytoma. Biochem Biophys Res Commun 1993;192:553–60.
6 Kim W, Moon SO, Sung MJ, Kim SH, Lee S, So JN, Park SK. Angiogenic role of adrenomedullin through activation of Akt, mitogen-activated protein kinase, and focal adhesion kinase in endothelial cells. FASEB J 2003;17:1937–9.
7 Tokunaga N, Nagaya N, Shirai M, Tanaka E, Ishibashi-Ueda H, Harada-Shiba M, Kanda M, Ito T, Shimizu W, Tabata Y, Uematsu M, Nishigami K, Sano S, Kangawa K, Mori H. Adrenomedullin gene transfer induces therapeutic angiogenesis in a rabbit model of chronic hind limb ischemia: Benefits of a novel nonviral vector, gelatin. Circulation 2004;109:526–31.
8 Iimuro S, Shindo T, Moriyama N, Amaki T, Niu P, Takeda N, Iwata H, Zhang Y, Ebihara A, Nagai R. Angiogenic effects of adrenomedullin in ischemia and tumor growth. Circ Res 2004;95:415–23.
9 Takahashi M, Suzuki E, Oba S, Nishimatsu H, Kimura K, Nagano T, Nagai R, Hirata Y. Adipose tissue-derived stem cells inhibit neointimal formation in a paracrine fashion in rat femoral artery. Am J Physiol Heart Circ Physiol 2010;298:H415–23.
10 Davis S, Aldrich TH, Jones PF, Acheson A, Compton DL, Jain V, Ryan TE, Bruno J, Radziejewski C, Maisonpierre PC, Yancopoulos GD. Isolation of angiopoietin-1, a ligand for the tie2 receptor, by secretion-trap expression cloning. Cell 1996;87:1161–9.
11 Ryu JK, Cho CH, Shin HY, Song SU, Oh SM, Lee M, Piao S, Han JY, Kim IH, Koh GY, Suh JK. Combined angiopoietin-1 and vascular endothelial growth factor gene transfer restores cavernous angiogenesis and erectile function in a rat model of hypercholesterolemia. Mol Ther 2006;13:705–15.
12 Zhao Q, Egashira K, Hiasa K, Ishibashi M, Inoue S, Ohtani K, Tan C, Shibuya M, Takeshita A, Sunagawa K. Essential role of vascular endothelial growth factor and Flt-1 signals in neointimal formation after periadventitial injury. Arterioscler Thromb Vasc Biol 2004;24:2284–9.
13 Ohtani K, Egashira K, Hiasa K, Zhao Q, Kitamoto S, Ishibashi M, Usui M, Inoue S, Yonemitsu Y, Sueishi K, Sata M, Shibuya M, Sunagawa K. Blockade of vascular endothelial growth factor suppresses experimental restenosis after intraluminal injury by inhibiting recruitment of monocyte lineage cells. Circulation 2004;110:2444–52.
14 Sawano A, Iwai S, Sakurai Y, Ito M, Shitara K, Nakahata T, Shibuya M. Flt-1, vascular endothelial growth factor receptor 1, is a novel cell surface marker for the lineage of monocyte-macrophages in humans. Blood 2001;97:785–91.
15 Shibuya M. Structure and function of VEGF/VEGF-receptor system involved in angiogenesis. Cell Struct Funct 2001;26:25–35.
16 Nishimatsu H, Hirata Y, Hayakawa H, Nagata D, Satonaka H, Suzuki E, Horie S, Takeuchi T, Ohta N, Homma Y, Minowada S, Nagai R, Kawabe K, Kitamura T. Effects of intracavernous administration of adrenomedullin on erectile function in rats. Peptides 2001;22:1913–8.
17 Suzuki E, Nagata D, Yoshizumi M, Kakoki M, Goto A, Omata M, Hirata Y. Reentry into the cell cycle of contact-inhibited vascular endothelial cells by a phosphatase inhibitor: Possible involvement of extracellular signal-regulated kinase and phosphatidylinositol 3-kinase. J Biol Chem 2000;275:3637–44.
18 Suzuki E, Nishimatsu H, Satonaka H, Walsh K, Goto A, Omata M, Fujita.T, Nagai R, Hirata Y. Angiotensin II induces myocyte enhancer factor 2- and calcineurin/nuclear factor of activated t cell-dependent transcriptional activation in vascular myocytes. Circ Res 2002;90:1004–11.
19 Takahashi M, Suzuki E, Kumano S, Oba S, Sato T, Nishimatsu H, Kimura K, Nagano T, Hirata Y. Angiopoietin-1 mediates adipose tissue-derived stem cell-induced inhibition of neointimal formation in rat femoral artery. Circ J 14 Mar 2013 [Epub ahead of print] doi: 10.1253/circj.CJ-12-0930.
20 Wespes E, Sattar AA, Golzarian J, Wery D, Daoud N, Schulman CC. Corporeal veno-occlusive dysfunction: Predominantly intracavernous muscular pathology. J Urol 1997;157:1678–80.
21 Garban H, Marquez D, Cai L, Rajfer J, Gonzalez-Cadavid NF. Restoration of normal adult penile erectile response in aged rats by long-term treatment with androgens. Biol Reprod 1995;53:1365–72.
22 Bakircioglu ME, Sievert KD, Nunes L, Lau A, Lin CS, Lue TF. Decreased trabecular smooth muscle and caveolin-1 expression in the penile tissue of aged rats. J Urol 2001;166:734–8.
23 Karvinen H, Pasanen E, Rissanen TT, Korpisalo P, Vahakangas E, Jazwa A, Giacca M, Yla-Herttuala S. Long-term VEGF—A expression promotes aberrant angiogenesis and fibrosis in skeletal muscle. Gene Ther 2011;18:1166–72.
24 Lin SL, Chang FC, Schrimpf C, Chen YT, Wu CF, Wu VC, Chiang WC, Kuhnert F, Kuo CJ, Chen YM, Wu KD, Tsai TJ, Duffield JS. Targeting endothelium-pericyte cross talk by inhibiting VEGF receptor signaling attenuates kidney microvascular rarefaction and fibrosis. Am J Pathol 2011;178:911–23.
25 Jin HR, Kim WJ, Song JS, Piao S, Choi MJ, Tumurbaatar M, Shin SH, Yin GN, Koh GY, Ryu JK, Suh JK. Intracavernous delivery of a designed angiopoietin-1 variant rescues erectile function by enhancing endothelial regeneration in the streptozotocin-induced diabetic mouse. Diabetes 2011;60:969–80.
26 Kim W, Moon SO, Lee SY, Jang KY, Cho CH, Koh GY, Choi KS, Yoon KH, Sung MJ, Kim DH, Lee S, Kang KP, Park SK. COMP-angiopoietin-1 ameliorates renal fibrosis in a unilateral ureteral obstruction model. J Am Soc Nephrol 2006;17:2474–83.
27 Kim I, Moon SO, Park SK, Chae SW, Koh GY. Angiopoietin-1 reduces VEGF-stimulated leukocyte adhesion to endothelial cells by reducing ICAM-1, VCAM-1, and E-selectin expression. Circ Res 2001;89:477–9.
28 Gu H, Cui M, Bai Y, Chen F, Ma K, Zhou C, Guo L. Angiopoietin-1/Tie2 signaling pathway inhibits lipopolysaccharide-induced activation of raw264.7 macrophage cells. Biochem Biophys Res Commun 2010;392:178–82.
29 Zhang JJ, Yoshida H, Chao L, Chao J. Human adrenomedullin gene delivery protects against cardiac hypertrophy, fibrosis, and renal damage in hypertensive dahl salt-sensitive rats. Hum Gene Ther 2000;11:1817–27.
30 Niu P, Shindo T, Iwata H, Iimuro S, Takeda N, Zhang Y, Ebihara A, Suematsu Y, Kangawa K, Hirata Y, Nagai R. Protective effects of endogenous adrenomedullin on cardiac hypertrophy, fibrosis, and renal damage. Circulation 2004;109:1789–94.
31 Nagae T, Mori K, Mukoyama M, Kasahara M, Yokoi H, Suganami T, Sawai K, Yoshioka T, Koshikawa M, Saito Y, Ogawa Y, Kuwabara T, Tanaka I, Sugawara A, Kuwahara T, Nakao K. Adrenomedullin inhibits connective tissue growth factor expression, extracellular signal-regulated kinase activation and renal fibrosis. Kidney Int 2008;74:70–80.

32 Ismail NS, Pravda EA, Li D, Shih SC, Dallabrida SM. Angiopoietin-1 reduces h(2)o(2)-induced increases in reactive oxygen species and oxidative damage to skin cells. J Invest Dermatol 2010;130:1307–17.
33 Kim SM, Kim JY, Lee S, Park JH. Adrenomedullin protects against hypoxia/reoxygenation-induced cell death by suppression of reactive oxygen species via thiol redox systems. FEBS Lett 2010;584:213–8.
34 Long T, Liu G, Wang Y, Chen Y, Zhang Y, Qin D. TNF-alpha, erectile dysfunction, and NADPH oxidase-mediated ros generation in corpus cavernosum in high-fat diet/streptozotocin-induced diabetic rats. J Sex Med 2012;9:1801–14.
35 Li M, Zhuan L, Wang T, Rao K, Yang J, Quan W, Liu J, Ye Z. Apocynin improves erectile function in diabetic rats through regulation of NADPH oxidase expression. J Sex Med 2012;9:3041–50.

Supporting Information

Additional Supporting Information may be found in the online version of this article at the publisher's website:

Figure S1 Blood glucose levels before and after adenoviral infection. Casual blood glucose levels were measured in each group 4 weeks after STZ injection (before adenoviral injection: white boxes) and 10 weeks after STZ injection (4 weeks after adenoviral injection: black boxes). Casual blood glucose levels were also measured in age-matched positive control rats (PC: dotted box). †: $P < 0.05$ vs. positive control rats. N = 6 in each group.

Adrenomedullin and Angiopoietin-1 Additively Restore Erectile Function in Diabetic Rats: Comparison with the Combination Therapy of Vascular Endothelial Growth Factor and Angiopoietin-1

Hiroaki Nishimatsu, MD, PhD,* Etsu Suzuki, MD, PhD,† Akira Nomiya, MD,* Aya Niimi, MD,* Motofumi Suzuki, MD, PhD,* Tetsuya Fujimura, MD, PhD,* Hiroshi Fukuhara, MD, PhD,* and Yukio Homma, MD, PhD*

*The Department of Urology, Faculty of Medicine, University of Tokyo, Tokyo, Japan; †Institute of Medical Science, St. Marianna University School of Medicine, Kawasaki, Japan

DOI: 10.1111/jsm.12177

ABSTRACT

Introduction. Erectile dysfunction (ED) is a major health problem. We have shown that adrenomedullin (AM) restores erectile function in diabetic rats.

Aim. The aim of this study is to explore a better treatment for ED, we examined whether combination of AM and angiopoietin-1 (Ang-1) was more effective to treat ED than treatment with AM alone or Ang-1 alone. We also compared the effect of the combination therapy with that of treatment with vascular endothelial growth factor-A (VEGF-A).

Methods. Male Wistar rats were injected with streptozotocin (STZ) to induce diabetes. Adenoviruses expessing AM (AdAM), Ang-1 (AdAng-1), and VEGF-A (AdVEGF-A) were injected into the penis 6 weeks after STZ administration. Erectile function, penile histology, and protein expression were analyzed 4 weeks after the injection of the adenoviruses.

Main Outcome Measures. Intracavernous pressure and mean arterial pressure were measured to evaluate erectile function. The morphology of the penis was analyzed by Elastica van Gieson stain and immunohistochemistry. The expression of α-smooth muscle actin (SMA), VE-cadherin and type I collagen was assessed by Western blot analysis.

Results. Infection with AdAM plus AdAng-1 more effectively restored erectile function than infection with AdAM alone or AdAng-1 alone. This combination therapy restored erectile function to a level similar to that observed in the age-matched Wistar rats. Expression of SMA and VE-cadherin increased more significantly in the AdAM plus AdAng-1-treated group than in the AdAM- or AdAng-1-treated group. Although AdVEGF-A infection restored erectile function significantly, it also caused enlargement of the trabeculae of the cavernous body, aberrant angiogenesis, and overproduction of type I collagen.

Conclusions. These results suggested that combination therapy with AM and Ang-1 potently restored erectile function and normal morphology of the cavernous body compared with VEGF-A administration. This combination therapy will be useful to treat ED patients with a severely damaged cavernous body. **Nishimatsu H, Suzuki E, Nomiya A, Niimi A, Suzuki M, Fujimura T, Fukuhara H, and Homma Y. Adrenomedullin and angiopoietin-1 additively restore erectile function in diabetic rats: Comparison with the combination therapy of vascular endothelial growth factor and angiopoietin-1. J Sex Med 2013;10:1707–1719.**

Key Words. Erectile Dysfunction; Adrenomedullin; Angiopoietin-1; Vascular Endothelial Growth Factor; Diabetes And Erectile Function

Hiroaki Nishimatsu and Etsu Suzuki contributed equally to this work.

Introduction

Erectile dysfunction (ED) is a major health problem that affects more than 10 million of the Japanese male population. It is estimated to affect approximately 75% of male patients with diabetes [1]. Although selective phosphodiesterase type 5 inhibitors (PDE-5) are widely used to treat ED, PDE-5 are less effective in patients with diabetes [2,3], probably because the cavernous body is severely damaged in these patients. To treat ED in the elderly population and in patients with diabetes whose cavernous body is profoundly damaged, it is necessary to explore a novel method to regenerate the cavernous body.

We have shown that administration of adipose tissue-derived stem cells (ASC), which are stem cells derived from subcutaneous adipose tissue, regenerated the cavernous body and restored erectile function in diabetic rats [4]. We have also demonstrated that ASC regenerated the cavernous body by secreting cytokines that stimulate angiogenesis rather than by being integrated in the cavernous body. Furthermore, we have shown that adrenomedullin (AM), a vasoactive peptide that has potent natriuretic, vasorelaxant, and proangiogenic activities [5–8], was produced by ASC and mediated ASC-induced restoration of erectile function [4]. Although AM was effective in restoring erectile function, its effect was apparently weaker than that of ASC administration [4]. It is therefore easily speculated that the combination of several cytokines that ASC produce will further improve erectile function. During the screening of cytokines that ASC produce, we found that angiopoietin-1 (Ang-1) was produced especially when ASC were cultured in medium that contains growth factors for vascular endothelial cells (VECs) [9]. Due to the fact that Ang-1 is also a potent proangiogenic factor [10], it is tempting to speculate that AM and Ang-1 will cooperatively stimulate the regeneration of the cavernous body.

Vascular endothelial growth factors (VEGF) are essential for vasculogenesis and have a potent proangiogenic activity. Among the VEGF family, VEGF-A is the major player in angiogenesis. It is therefore expected that VEGF-A also helps to regenerate the cavernous body by stimulating angiogenesis in the penis. In fact, it was reported that administration of VEGF-A restored erectile function [11]. However, overexpression of VEGF-A causes harmful effects in other organs. In the vascular restenosis model, VEGF-A was expected to stimulate reendothelialization and in turn inhibit neointimal formation after mechanical injury to the vascular endothelial layer via stimulating migration and proliferation of VECs. Contrary to this expectation, several reports showed that blockade of the endogenous VEGF family rather than stimulation of VEGF-A expression inhibited neointimal formation [12,13]. There are several possible mechanisms by which VEGF-A stimulates neointimal formation. First, VEGF-A stimulates the migration of monocytes/macrophages, because monocytes/macrophages express Flt-1, the type 1 receptor for VEGF [14]. VEGF-A may also stimulate the migration of monocytes/macrophages by increasing the permeability of blood vessels [15]. Second, VEGF-A stimulates the migration and/or proliferation of vascular smooth muscle cell (VSMC)-like cells that reside in the neointimal layer, because these VSMC-like cells reportedly express Flt-1 [12,13]. Thus, some proangiogenic factors such as VEGF-A have proinflammatory activities. It is therefore important to choose an appropriate combination of proangiogenic factors to stimulate regeneration of the cavernous body.

In this study, we examined whether administration of AM and Ang-1 would cooperatively restore erectile function by stimulating regeneration of VECs and VSMCs in the cavernous body. We also compared the effect of coadministration of AM and Ang-1 with that of VEGF-A and/or Ang-1.

Materials and Methods

Reagents

Anti-VE-cadherin antibody used for Western blot analysis, anti-α-smooth muscle actin (SMA) antibody, and anti-β-actin antibody were purchased from Santa-Cruz Biotechnology Inc. (Santa-Cruz, CA, USA). Anti-VE-cadherin antibody used for immunohistochemical analysis was obtained from LifeSpan BioSciences (Seattle, WA, USA). Anti-type I collagen antibody was purchased from Abcam (Tokyo, Japan).

Cell Culture

NRK-52E cells, a cell line derived from rat renal tubular cells, and HEK293 cells were obtained from ATCC (Manassas, VA, USA) and cultured in Dulbecco's modified Eagle medium (DMEM) containing 5% fetal bovine serum (FBS).

Animal Experiments

All procedures involving experimental animals were approved by the institutional committee for

animal research of the Tokyo University. Streptozotocin (STZ; 50 mg/kg body weight; Sigma-Aldrich) was dissolved in citrate buffer (pH 4.5) and injected in the tail vein of male Wistar rats (6 weeks old; Charles River, Wilmington, MA, USA). Blood glucose level was measured 4 weeks later to confirm that these rats had become diabetic. Adenovirus suspension diluted in saline up to 200 μL was injected into the penis 6 weeks after STZ injection. Adenovirus expressing green fluorescent protein (AdGFP), adrenomedullin (AdAM), angiopoietin-1 (AdAng-1), or vascular endothelial growth factor-A (AdVEGF-A) was injected into the penis (10 rats per group). Furthermore, AdAM plus AdAng-1 or AdVEGF-A plus AdAng-1 was injected into the penis (10 rats per group). Four weeks after adenovirus injection, rats (16 weeks old) were subjected to intracavernous pressure (ICP) measurement. The penis was also harvested for histochemical analysis and Western blot analysis at this time point. The penises isolated from six rats per group were subjected to ICP measurements, and then Western blot analysis. The penises isolated from the remaining four rats per group were used for histochemical analysis. AdGFP-injected diabetic rats were used as negative controls, and age-matched nondiabetic Wistar rats were used as positive controls in this study.

ICP Measurement

ICP measurement was performed in the same way as we previously reported [16]. Rats were anesthetized with ketamine (100 mg/kg body weight) injected intraperitoneally. The left carotid artery was exposed and cannulated with a PE-50 polyethylene tube to continuously monitor mean arterial pressure (MAP). The penis was denuded of skin and the pelvic nerve and cavernous nerve were isolated. The right cavernous nerve was hooked with stainless platinum bipolar electrodes (Unique Medical Co., Tokyo, Japan) and connected to a nerve stimulator (Nihon Kohden Co., Tokyo, Japan). Unilateral electrical field stimulation of the cavernous nerve was performed for 10 seconds using a square wave stimulator. The magnitude of the electrical voltage was 5.0 V with a pulse duration of 2 msec, and the frequency of the stimulation was 20 Hz. The right cavernous body was cannulated with a 23-gauge needle connected to a pressure transducer to continuously monitor ICP. Area under the curve (AUC) of ICP traces as well as the ratio of peak ICP to MAP (ICP/MAP) were used to evaluate erectile function. AUC was measured from the point when ICP started to increase from the base line values after electrical stimulation to the point when ICP decreased and reached a plateau. ICP × time was integrated every 0.2 second to calculate AUC.

Protein Extraction and Western Blot Analysis

The penis was homogenized in a cell lysis buffer (50 mM Tris-HCl [pH 8.0], 150 mM NaCl, 1% NP-40) containing 2 μg/mL aprotinin, 2 μg/mL leupeptin, and 1 mM phenylmethylsulfonyl fluoride. Western blot analysis was performed as previously described [17]. To detect type I collagen, we performed electrophoresis under nondenatured conditions, because the anti-type I collagen antibody used in this experiment recognizes nondenatured protein. Sodium dodecyl sulfate (SDS) and β-mercaptoethanol were left out from the loading dye, and samples were loaded on polyacrylamide gel without boiling. SDS was also omitted from the polyacrylamide gel, electrophoresis buffer, and transfer buffer. The expression of VE-cadherin, SMA, and type I collagen was normalized by calculating the ratio of the expression of those proteins to that of β-actin.

RNA Extraction and Real Time PCR Analysis

Total RNA was extracted using TRIZOL Reagent (Gibco-BRL, Rockville, MD, USA) according to the instructions provided by the manufacturer. To extract total RNA from the rat penis, the penis was homogenized in the TRIZOL Reagent. Total RNA was subjected to reverse transcription using a ReverTra Ace qPCR RT Kit (Toyobo, Osaka, Japan). Expression of rat AM, Ang-1, VEGF-A and glyceraldehyde 3-phosphate dehydrogenase (GAPDH) was examined by real-time PCR using an SYBR Green dye (Thunderbird SYBR qPCR Mix, Toyobo). Primers used were as follows:

RatAMsense, 5′-GCAGTTCCGAAAGAAGTG GAAT-3′
RatAMantisense, 5′-GCTGCTGGACGCTTGT AGTTC-3′
RatAng-1sense, 5′-CAGGAGGTTGGTGGTT TGATG-3′
RatAng-1antisense, 5′-TTTGCCCTGCAGTG TAGAACATT-3′
RatVEGF-Asense, 5′-GAGTATATCTTCAAGC CGTCCTGTGT-3′
RatVEGF-Aantisense, 5′-TCCAGGGCTTCAT CATTGC-3′
RatGAPDHsense, 5′-GTATGACTCTACCCAC GGCAAGT-3′
RatGAPDHantisense, 5′-TTCCCGTTGATGA CCAGCTT-3′

Real-time PCR was performed using an ABI PRISM 7000 sequence detection system (Applied Biosystems, Foster City, CA, USA). To confirm that no significant amounts of primer dimers were formed, dissociation curves were analyzed.

Histochemistry

The penis was fixed by perfusing it with 4% paraformaldehyde and then processed for paraffin embedding. Cross sections (5 μm) were cut, deparaffinized, rehydrated, and subjected to Elastica van Gieson stain to visualize collagen and elastin fibers in the trabeculae of the cavernous body. For immunohistochemistry, sections were incubated with a primary antibody reactive to VE-cadherin and SMA. Sections were then incubated with biotinylated secondary antibody and finally horseradish peroxidase-labeled streptavidin according to the instructions provided by the manufacturer (DAKO, Cambridgeshire, UK).

Construction of Adenovirus that Expresses VEGF-A

Replication-defective adenovirus that expresses rat VEGF-A was constructed according to the method described previously using an AdMax kit (Microbix Biosystems Inc., Ontario, Canada) [18]. The coding region of rat VEGF-A was amplified by PCR and subcloned into the pDC516 vector. The primer sequences used for PCR were as follows:

RatVEGF-Asense primer: 5′-ATGAACTTTCT GCTCTCTTGGGT-3′
RatVEGF-Aantisense primer: 5′-TCACCGCCT TGGCTTGTCACAT-3′

The result of DNA sequencing analysis showed that the VEGF-A isolated in this study was rat VEGF-A164 corresponding to human VEGF-A165, in which amino acids 141 to 164 were missing by alternative splicing. The expression plasmid pDC516 that expresses rat VEGF-A164 was cotransfected into HEK293 cells with pBHGfrtdelE13FLP to construct an adenovirus expressing rat VEGF-A164 (AdVEGF-A). Construction of adenovirus that expresses rat AM (AdAM) [4] and rat Ang-1 (AdAng-1) [19] has been reported elsewhere. Recombinant adenovirus that expresses GFP (AdGFP) was obtained from Quantum Biotechnologies (Montreal, Canada). These adenoviruses were purified before in vivo use with the Adeno-X Maxi Purification Kit (Takara Bio Inc., Tokyo, Japan) according to the manufacturer's instructions.

Enzyme-Linked Immunosorbent Assay

Rat VEGF-A in culture medium was measured with an enzyme-linked immunosorbent assay kit (Abcam, Cambridge, UK) according to the methods provided by the manufacturer.

Statistical Analysis

The values are expressed as the mean ± SEM. Statistical analyses were performed using analysis of variance followed by the Student–Neumann–Keuls test. Differences with a P value of <0.05 were considered statistically significant.

Results

Characterization of AdVEGF-A

We first examined whether AdVEGF-A-infected cells produced VEGF-A using an ELISA kit for rat VEGF-A. We infected NRK-52E cells with AdVEGF-A and measured the VEGF-A content in the culture medium. Although we expected that the NRK-52E cells did not produce endogenous VEGF-A, they produced a significant amount of VEGF-A (Figure 1). However, AdVEGF-A-infected NRK-52E cells produced a more significant amount of VEGF-A (approximately fivefolds) compared with the AdGFP-infected and noninfected control NRK-52E cells, confirming that the AdVEGF-A used in this study produced VEGF-A protein. Previous studies have reported that

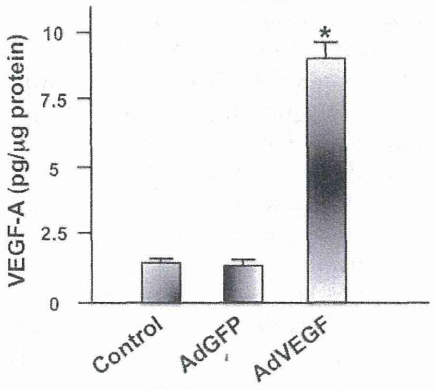

Figure 1 Production of VEGF-A by AdVEGF-A. NRK-52E cells were cultured in 24-well plates and infected with AdGFP or AdVEGF-A for 3 days. After washing the wells with phosphate-buffered saline (PBS), medium was replaced with serum-free DMEM, and incubated for 2 hours. VEGF-A accumulated in the medium was measured with an ELISA kit. Noninfected NRK 52E cells were also used as the control (Control). *: $P < 0.001$ vs. control and AdGFP infection ($n = 6$ each)

AdAM produces rat AM protein [4] and AdAng-1 produces rat Ang-1 protein [19].

Expression of Adenovirus in the Penis

To confirm that adenovirus injected into the penis expressed AM, Ang-1, and VEGF-A in the penis, AdGFP, AdAM, AdAng-1, or AdVEGF-A were injected into the penis of STZ-induced diabetic rats, and the penis was harvested 7 days after adenoviral infection for real-time PCR analysis. Penises injected with AdAM, AdAng-1, and AdVEGF-A expressed significantly higher amounts of AM, Ang-1, and VEGF-A, respectively, than those injected with AdGFP. This result suggested that adenovirus injected into the penis remained and those cytokines were therefore expressed (Figure 2).

Effects of Administration of AdAM, AdAng-1, and AdVEGF-A on ICP

We infected AdAM, AdAng-1, and AdVEGF-A into the cavernous body at the glans of STZ-induced diabetic rats and measured ICP 4 weeks after the infection. We confirmed in a previous study that AdGFP infection did not affect ICP or histology in STZ-induced diabetic rats [4]. We analyzed not only ICP and AUC of ICP traces, but also Tmax and $T_{1/2}$. Tmax is defined as a period from when ICP starts to increase after electrical stimulation to when ICP reaches maximal level (Figure 3A). $T_{1/2}$ is defined as a period from when ICP starts to increase after electrical stimulation to when ICP decreases to the 50% level of its maximal value (Figure 3A). Infection of the penis with AdAM, AdAng1, AdAM plus AdAng-1, AdVEGF-A, and AdVEGF-A plus AdAng-1 all restored ICP significantly compared with AdGFP infection in the diabetic rats (Figure 3B). Infection with AdAM plus AdAng-1, AdVEGF-A, and AdVEGF-A plus AdAng-1 restored ICP to a level similar to that observed in age-matched Wistar rats (positive control). Infection with AdAM, AdAng1, AdAM plus AdAng-1, AdVEGF-A, and AdVEGF-A plus AdAng-1 also increased AUC of the ICP traces significantly compared with AdGFP infection in the diabetic rats (Figure 3C). Infection with AdAM plus AdAng-1 restored AUC most significantly. Tmax in the AdGFP-infected group was significantly elongated compared with the positive control group (Figure 3D), and Tmax in the AdAng-1-infected group tended to be retarded, and there was no significant difference in Tmax between the AdGFP-infected group and the AdAng-1-infected group. These results suggested

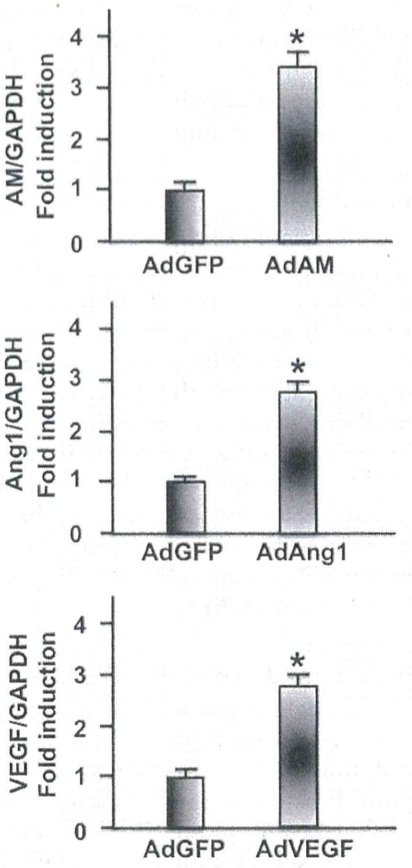

Figure 2 Expression of adenovirus in the penis. AdAM, AdAng-1, or AdVEGF-A was injected into the penis of STZ-induced diabetic rats, and the penis was isolated 7 days after adenoviral injection for real-time PCR analysis. AdGFP was also injected into the penis as a negative control. Expression of AM, Ang-1, and VEGF-A (VEGF) was normalized by that of GAPDH ($n = 4$ each). *: $P < 0.01$ vs. AdGFP infection

that blood filling into the cavernous body occurred more slowly in the AdGFP-infected and AdAng-1-infected diabetic rats than the age-matched Wistar rats. Interestingly, Tmax in the AdVEGF-A- and AdVEGF-A plus AdAng-1-infected groups was significantly shortened compared with the positive control group, suggesting that blood filling into the cavernous body occurred faster in these groups than the positive control. Tmax in the AdAM- and AdAM plus AdAng-1-infected groups was similar to that in the positive control group. $T_{1/2}$ in the AdGFP- and AdAng-1-infected groups was significantly elongated compared with the positive control (Figure 3E). $T_{1/2}$ in the AdVEGF-A- and AdVEGF-A plus AdAng-1-infected groups was significantly shortened

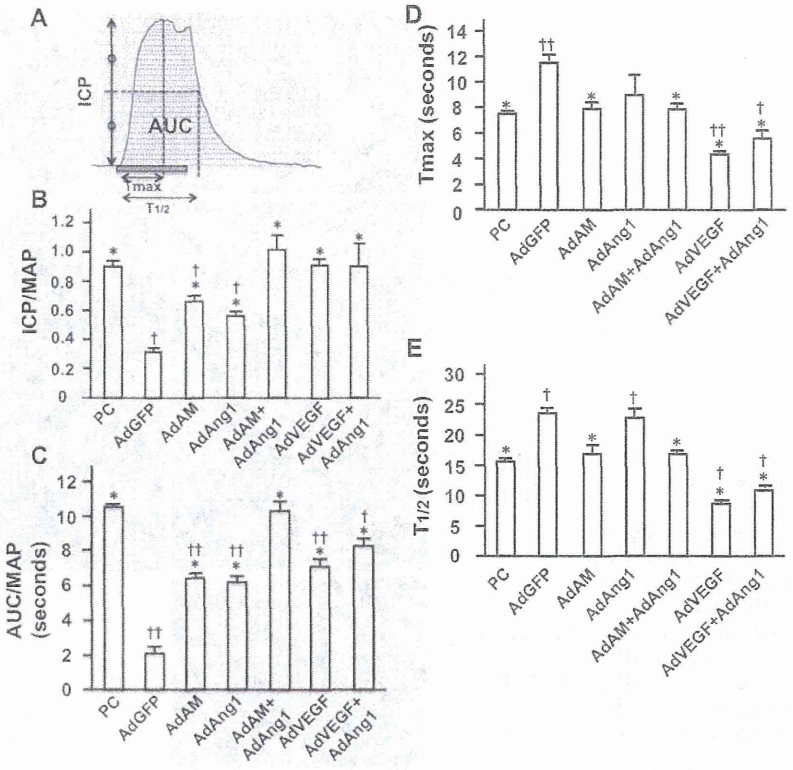

Figure 3 Effects of AdAM, AdAng-1, and AdVEGF-A infection on erectile function. These adenoviruses were infected into the cavernous body of STZ-induced diabetic rats. Age-matched Wistar rats were used as the positive control (PC). (A) Schematic representation of ICP traces. The dashed box indicates the timing and duration of electrical stimulation. The dotted area represents AUC. Tmax was defined as the period from when ICP started to rise to when ICP reached its peak level. $T_{1/2}$ was defined as the period from when ICP started to rise to when it fell to the 50% of its peak level. (B) Bar graphs comparing ICP/MAP among the groups ($n = 6$ each). *: $P < 0.001$ vs. AdGFP infection and †: $P < 0.001$ vs. PC. (C) Bar graphs comparing AUC/MAP among the groups ($n = 6$ each). *: $P < 0.001$ vs. AdGFP infection, and † and ††: $P < 0.01$ and $P < 0.001$, respectively, vs. PC. (D) Bar graphs comparing Tmax among the groups ($n = 6$ each). *: $P < 0.001$ vs. AdGFP infection and † and ††: $P < 0.05$ and $P < 0.001$, respectively vs. PC. (E) Bar graphs comparing $T_{1/2}$ among the groups ($n = 6$ each). *: $P < 0.001$ vs. AdGFP infection and †: $P < 0.001$ vs. PC

compared with the positive control group. $T_{1/2}$ in the AdAM- and AdAM plus AdAng-1-infected groups was similar to that in the positive control group. Collectively, infection with AdAM, AdAng1, AdAM plus AdAng-1, AdVEGF-A, and AdVEGF-A plus AdAng-1 all restored erectile function significantly. The effect of AdAM plus AdAng-1 infection was most significant, and the erectile function in this group was similar to that in the positive control group. The speed of rise and fall of ICP after electrical stimulation was decreased in the AdGFP- and AdAng-1-infected groups compared with the positive control group. The speed increased in the AdVEGF-A- and AdVEGF-A plus AdAng-1-infected groups compared with the positive control group. The speed did not change significantly in the AdAM- or AdAM plus AdAng-1-infected group compared with the positive control group. Thus, ICP traces in the AdAM plus AdAng-1-infected group mostly mimicked those in the positive control group.

Effects of Administration of AdAM, AdAng-1, and AdVEGF-A on Histology of the Cavernous Body

To examine the mechanisms by which these adenoviral infections restored erectile function, we examined the morphology of the cavernous body by Elastica van Gieson staining. The trabeculae of the cavernous body at the root of the penis in the AdGFP-infected diabetic rats were smaller than those in the positive control Wistar rats (Figure 4). Infection with AdAM and/or AdAng-1 restored the size of the trabeculae of the cavernous body.

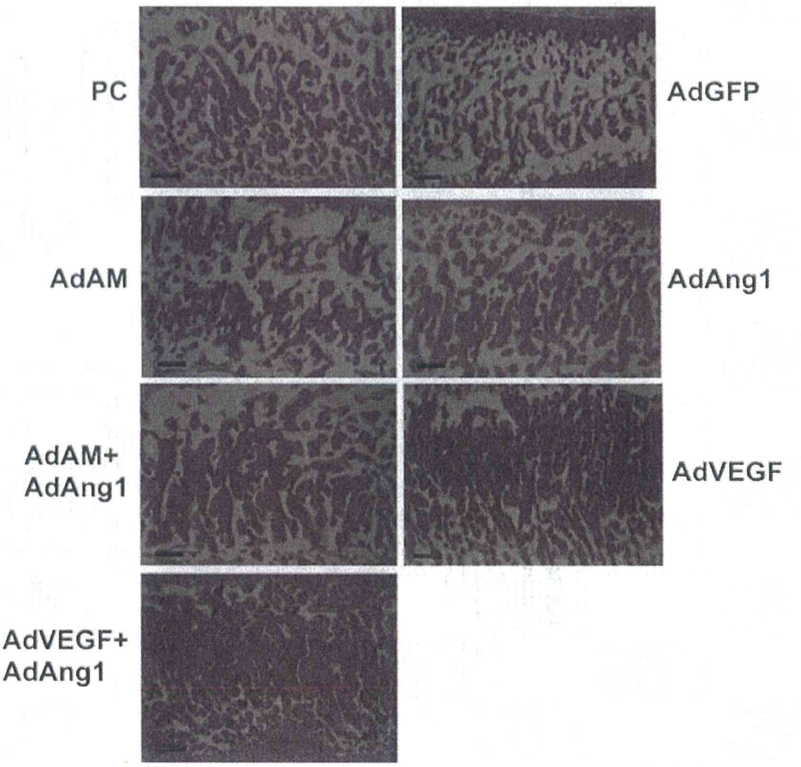

Figure 4 Histological analysis of the cavernous body after adenoviral infection. Elastica van Gieson staining of the cavernous body isolated from age-matched Wistar rats (PC), and STZ-induced diabetic rats infected with AdGFP, AdAM, AdAng-1, AdAM plus AdAng-1, AdVEGF-A (AdVEGF), and AdVEGF-A plus AdAng-1. The histology of the root portion of the penis (longitudinal section) is shown. Bars are 300 μm.

Interestingly, the trabeculae of the cavernous body were rather enlarged and densely distributed in the cavernous body in the AdVEGF-A- and AdVEGF-A plus AdAng-1-infected groups compared with the positive control group. We next examined the distribution of SMA and VE-cadherin by immunohistological analysis. The SMA layer around the trabeculae of the cavernous body in the AdGFP-infected diabetic rats looked thinner than that in the other adenovirus-infected groups and the positive control group (Figure 5). The VE-cadherin-positive endothelial layer around the trabeculae of the cavernous body was observed in all groups (Figure 6), and the ratios of trabeculae covered with VECs to those uncovered with VECs seemed to be similar among the groups, although the total amount of the endothelial layer might be different among the groups because the size and the density of the trabeculae of the cavernous body differed among the groups. Interestingly, we observed a VE-cadherin-positive tube-like structure in the trabeculae of the cavernous body in the AdVEGF-A-infected group (Figure 6), suggesting that an aberrant angiogenesis occurred in the AdVEGF-A-infected group.

Effects of Administration of AdAM, AdAng-1, and AdVEGF-A on the Expression of VE-Cadherin, SMA, and Type I Collagen

To quantify the expression of SMA and VE-cadherin, we performed Western blot analysis (Figure 7). Infection with AdAM or AdAng-1 increased SMA expression slightly but significantly compared with AdGFP infection. Infection with AdAM plus AdAng-1, AdVEGF-A, and AdVEGF-A plus AdAng-1 increased SMA expression more significantly, and the expression level was similar to that in the age-matched positive control group. Infection with AdAM or AdAng-1 significantly increased VE-cadherin expression compared with AdGFP infection. Infection with AdAM plus AdAng-1 increased VE-cadherin expression more significantly, and the expression reached a level similar to that in the positive control group. The expression of VE-cadherin in the AdVEGF-A- and AdVEGF-A plus AdAng-1-infected groups rather surpassed the expression level observed in the positive control. We also examined the expression of type I collagen as a marker to quantify the content of collagen fibers in the trabeculae of the cavernous body, because we found that the trabeculae were "hypertrophied" in

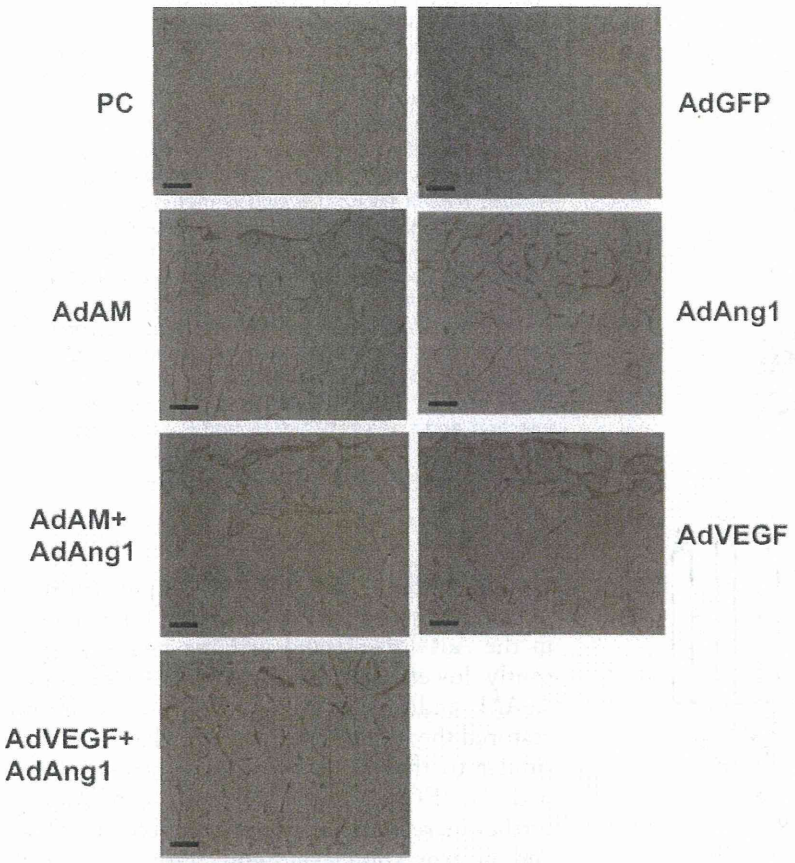

Figure 5 Immunohistochemical analysis of the cavernous body isolated from age-matched Wistar rats (PC) and STZ-induced diabetic rats infected with AdGFP, AdAM, AdAng-1, AdAM plus AdAng-1, AdVEGF-A (AdVEGF), and AdVEGF-A plus AdAng-1. SMA was stained to visualize the smooth muscle layer in the cavernous body. The longitudinal section of the cavernous body at the root of the penis is shown. Bars are 300 μm.

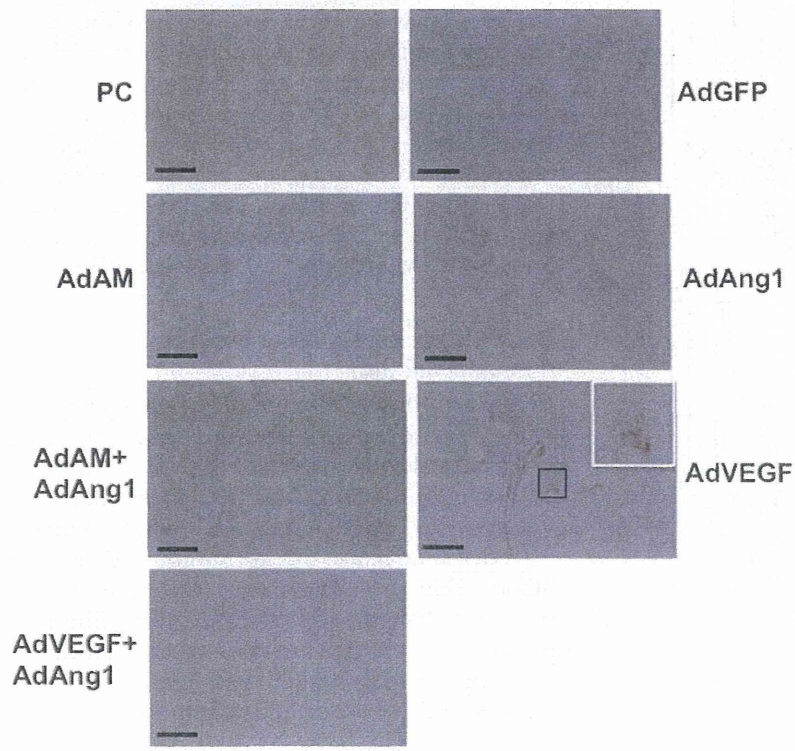

Figure 6 Immunohistochemical analysis of the cavernous body isolated from age-matched Wistar rats (PC) and STZ-induced diabetic rats infected with AdGFP, AdAM, AdAng-1, AdAM plus AdAng-1, AdVEGF-A (AdVEGF), and AdVEGF-A plus AdAng-1. VE-cadherin was stained to visualize the endothelial layer in the cavernous body. Area of aberrant angiogenesis observed in the trabeculae of the cavernous body of AdVEGF-A infected penis was boxed and enlarged in the white box. The longitudinal section of the cavernous body at the root of the penis is shown. Bars are 100 μm.

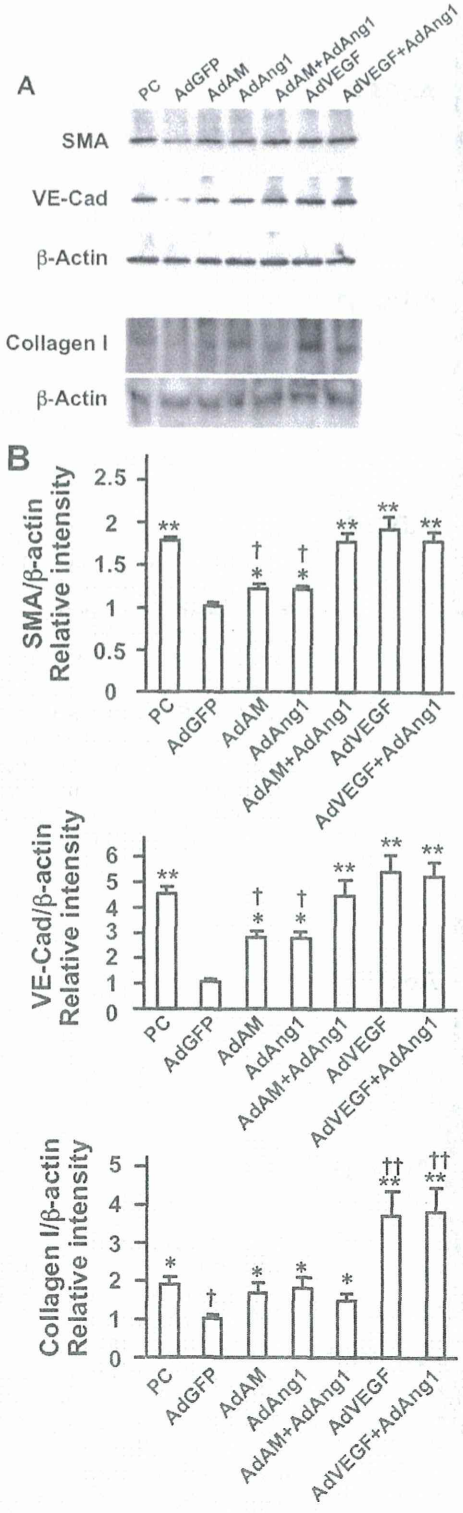

Figure 7 Western blot analysis of the expressions of SMA, VE-cadherin, and type I collagen in the penis. (A) AdGFP, AdAM, AdAng-1, AdAM plus AdAng-1, AdVEGF-A (AdVEGF), and AdVEGF-A plus AdAng-1 were infected in the cavernous body of STZ-treated diabetic rats, and the penis was isolated for protein extraction 4 weeks after adenoviral injection. Age-matched Wistar rats were used as the positive control (PC). The blotted membranes were incubated with anti-SMA antibody, anti-VE-cadherin antibody, and then anti-β-actin antibody as the internal control. To detect type I collagen, protein extracts were electrophoresed on nondenatured SDS polyacrylamide gels, and blotted membranes were incubated with anti-type I collagen antibody and then anti-β-actin antibody as the internal control. (B) Histograms showing relative intensity of the bands ($n = 4$ each). * and **: $P < 0.05$ and $P < 0.01$ vs. AdGFP infection, and † and ††: $P < 0.05$ and $P < 0.01$, respectively, vs. PC.

the AdVEGF-A- and AdVEGF-A plus AdAng-1-infected groups. Expression level of type I collagen in the AdGFP-infected diabetic rats was significantly lower than that in the positive control. AdAM and/or AdAng-1 infection significantly restored the expression of type I collagen to a level similar to that in the positive control. Infection with AdVEGF-A and AdVEGF-A plus AdAng-1 further increased the expression of type I collagen, and the expression level significantly exceeded that in the positive control. Collectively, these results suggested that the vascular networks of the cavernous sinus were poorly developed in the AdGFP-infected diabetic rats, and infection with AdAM, AdAng-1, and AdVEGF-A restored the networks significantly. However, AdVEGF-A infection induced an excess amount of angiogenesis and synthesis of collagen fibers, resulting in aberrant angiogenesis in the trabeculae of the cavernous body and "hypertrophy" of the trabeculae.

Blood Glucose Levels Before and After Adenoviral Infection

To confirm that adenoviral infection did not affect blood glucose levels, we measured the casual blood glucose levels 4 weeks after STZ injection (before adenoviral infection) and 10 weeks after STZ injection (4 weeks after adenoviral infection). Adenoviral infection did not significantly alter the blood glucose levels, and the diabetic rats remained diabetic after the infection. The blood glucose levels of adenovirus-infected diabetic rats were significantly higher than age-matched nondiabetic rats (16 weeks old) (Supporting Information Figure S1).